Abdominal Imaging

Published online: 3 July 2007

Abdom Imaging (2008) 33:371–380
DOI: 10.1007/s00261-007-9257-6

Female urinary incontinence: pathophysiology, methods of evaluation and role of MR imaging

Katarzyna J. Macura,[1] Rene R. Genadry[2]

[1]The Russell H. Morgan Department of Radiology and Radiological Sciences, Johns Hopkins University, Baltimore, MD 21287, USA
[2]Department of Gynecology and Obstetrics, Johns Hopkins University, Baltimore, MD 21287, USA

Abstract

Urinary incontinence (UI) is one of the most common conditions that cause a significant psychosocial and hygienic problem in an aging female population. In this article we focus on the sphincteric type of stress UI in women, review the anatomy of the urethral sphincter and its support mechanism, and discuss methods of the evaluation of urethral function. Stress UI is the functional consequence of an anatomical abnormality, urethral hypermobility (UH) and intrinsic sphincter deficiency (ISD). Imaging plays an adjunct role to urodynamics in the assessment of women with UI. MR imaging due to its superior soft tissue contrast resolution contributes many findings that are predictive of UH, such as abnormal descent of the bladder neck, disruption of periurethral ligaments and vaginal attachments, and defects within the levator ani muscle. In ISD, MR imaging may show foreshortening or thinning of the sphincter muscle and bladder neck insufficiency manifested by funneling. MR imaging is ideal to evaluate the anatomy of the bladder neck and urethra; functional implications correlate well with functional studies and make MR imaging central to understanding the causes of stress UI and its thorough evaluation.

Urinary incontinence (UI) is the involuntary loss of urine. In a female population, UI is one of the most common conditions that cause a significant psychosocial and hygienic problem [1]. UI can be caused by urinary bladder abnormalities, such as detrussor overactivity and low bladder compliance, and urethral sphincter abnormalities. The primary types of UI include: (a) stress incontinence, urine loss during physical activity that increases abdominal pressure (e.g., coughing, sneezing, laughing); (b) urge incontinence, urine loss with urgent need to void and involuntary bladder contraction (detrusor instability); (c) mixed—both stress and urge incontinence, (d) overflow incontinence, with constant dribbling of urine and bladder incompletely emptying. Of the several types of UI, stress UI is the most common in women. Some of the causes include loss of urethral compression and support after previous pelvic surgery, childbirth, or trauma, reduced sphincteric function in lumbosacral neurologic conditions, and because of aging with hypoestrogenic state. Urge incontinence is most common in the elderly and may be a sign of bladder infection. Overflow incontinence is more common in people with neurogenic disorders and older men with bladder outlet obstruction because of benign prostatic hypertrophy. In this article we focus on the sphincteric type of stress UI in women. Sphincteric incontinence is related to urethral hypermobility (UH) and intrinsic sphincter deficiency (ISD) [2]. The basic abnormality in UH is a weakness of pelvic floor support that results in a rotational descent of the vesical neck and urethra during increases in abdominal pressure. When the poorly supported posterior urethra continues its excursion away from the better supported anterior urethra, the urethrovesical junction opens concomitantly with its descent and UI ensues. In ISD, there is malfunction of the urethral sphincter, rather than pelvic floor defect, which leads to low urethra closure pressures. As a result of weakening of the sphincter, the vesical neck opens at rest or strain leading to UI symptoms [3]. The normal female urethra remains closed no matter what degree of stress (increase in intraabdominal pressure) or rotational descent is present.

Traditionally, studying the urethra and its supporting structures has been possible with procedures that indi-

Correspondence to: Katarzyna J. Macura; *email:* kmacura@jhmi.edu

rectly evaluate urethral anatomy and function. Cystourethroscopy assesses the urethral coaptation, which is the ability to close the urethral lumen, and the status of the mucosa. Neural control can be assessed with bladder and urethral sphincter electromyography (EMG). Videourodynamics combining urethral pressure measurements and urethrocystography have been used to assess the process of bladder filling and compliance, micturition, and urethral closure. Direct visualization of the urethral wall can be performed with ultrasound, using the transabdominal, translabial, transperineal, endovaginal, transrectal, or intraurethral approach [4–9], and with MR imaging. With its excellent soft tissue contrast and multiplanar acquisition, MR imaging enhances the ability to visualize the female urethra and periurethral tissues relevant to UI. Standard evaluation of the female urethra with MR involves the use of pelvic surface coils; however, endocavitary MR coils, endovaginal [10], endorectal [11], and intraurethral [12] have subsequently allowed MR imaging of the urethra with increased spatial resolution and high signal-to-noise ratio (SNR). With the increasing anatomical detail of urethral anatomy that can be visualized on MR imaging, our understanding of the morphological changes related to stress UI should improve, and it is expected that new methods for diagnosis and staging of urethral dysfunction will be devised.

In this article we review the anatomy of the female urethral sphincter and periurethral attachments that promote continence, and discuss methods of the evaluation of urethral morphology and function. We also illustrate the MR imaging findings in stress urinary incontinence related to UH and ISD in women.

Anatomy of urethra

The female urethra is about 3.5–4.5 cm long, with at least 2/3 of the proximal urethra positioned above the levator ani (pelvic diaphragm) level. The proximal 1/3 of the urethra is lined with transitional cell epithelium. The mid and distal urethra is lined with pseudo-stratified columnar epithelium. Infoldings of urothelial tissue with rich submucosal vascular plexuses, mucosal secretions, and urethral smooth muscle contribute to passive urethral closure (urethral coaptation and mucosal seal). The urethral sphincter muscle comprises involuntary inner smooth muscle, and the voluntary external sphincter (rhabdosphincter) comprises striated muscle. In the histologic study of paraurethral anatomy, DeLancey defined four segments along the urethral length between the internal urethral meatus and the external meatus [13]. MR imaging with its high soft tissue contrast resolution allows visualization of the urethra and supporting structures with great detail, and these four distinct portions of the urethra can be seen on imaging. The proximal 20% of the urethra is the intramural urethra which traverses the urinary bladder wall. As the urethra passes through the wall of the bladder, the muscle fibers (low intensity on T2-weighted imaging) of the detrusor extend as far as 20% of the urethral length below the internal urethral meatus (Fig. 1). The mid-40% of the urethra shows the smooth and striated muscles of the urethral sphincter. The striated urethral sphincter is divided into three components: (a) the urethral sphincter surrounding circularly the proximal and midurethra where the urethra is separable from the adjacent vaginal wall, (b) the urethrovaginal sphincter with fibers surrounding both the urethra and the vagina (Fig. 1), and (c) the compressor urethrae with fibers running from the ischiopubic rami and also originating from the perineal membrane itself to the anterior urethra, where they meet fibers from the opposite side forming a broad arcing muscle [14]. In the axial plane, T2-weighted images of the midurethra show a multilayered target appearance (Fig. 2). The inner smooth muscle layer (longitudinal and circumferential) [15] in a loose connective tissue matrix shows high signal intensity. The smooth muscle layer is thickest at the midurethral level and on the ventral side of the urethra. The outer layer of low-intensity tissue encircling the smooth muscle represents the striated urogenital sphincter muscle (rhabdosphincter) within a dense connective tissue layer (Fig. 2). The striated muscle is thicker on the ventral and lateral side of the urethra, and thinner on the dorsal side. On the transverse sections, the target-like appearance of the midurethra differs slightly at the upper, mid, and lower midurethra segments. The thickness of the smooth and striated muscle layers differs along the midurethral length, with the upper and mid-segments thicker than the lower segment [12]. Urethral sphincteric function depends on the integrity of the mucosa, submucosa, and smooth urethra muscle layers as well as the striated urethral sphincter responsible for compressing the urethra directly via its circular fibers (urethral and urethrovaginal portions) and for pulling it deeper into the anterior wall of the vagina through its arcing fibers of the compressor urethrae portion. In combination with the action of the pelvic diaphragm that elevates the bladder, the urethral sphincter assists in the elongation of the urethra. The urethral elongation has been found important in providing continence [14]. About 20% of the distal urethral length is embedded in the urogenital diaphragm supported by the compressor urethrae muscle and the urethrovaginal sphincter muscle [13]. The most distal 20% of the urethra below the pelvic floor level where the urethra passes between the vestibular bulbs and the bulbocavernosus muscle, is composed only of the fibrous tissue without any skeletal and smooth muscle component (Fig. 1).

Both pelvic muscles and fasciae determine the support of the urethra. The fascial attachments of the urethra connect the periurethral tissues and anterior vaginal wall to the arcus tendineus fascia pelvis and have been called the paravaginal fascial attachments.

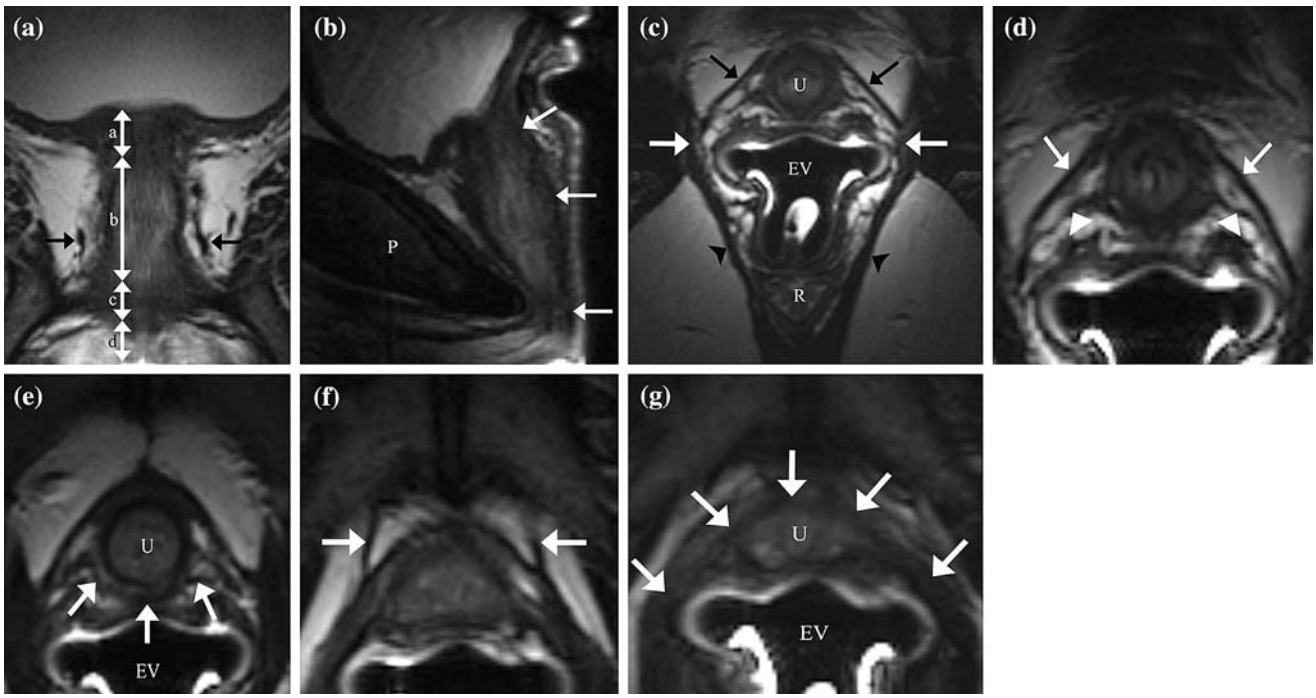

Fig. 1 A 34-year-old continent woman volunteer. Images obtained with endovaginal placement of MRInnervu coil (Medrad, Indianola, PA, USA) on 1.5T GE scanner (Signa LX, GE Medical Systems, Waukesha, WI, USA). **A** Coronal T2-weighted image (TR/TE 3,000/95 ms) shows four segments of the urethra, total length 4.5 cm, from proximal to distal: (*a*) intramural, bladder neck level 0.9 cm long, (*b*) midurethra where urethral sphincter has a multilayered appearance, with the inner hyperintense smooth muscle and outer hypointense striated muscle, is 1.8 cm, (*c*) urogenital diaphragm level, 0.9 cm long, and (*d*) distal urethra comprising fibrous tissue only, 0.9 cm long. Note end-on appearance of pubourethral ligaments (*arrows*) visualized parallel to the lower segment of urethra, just above the urogenital diaphragm. **B** Sagittal T2-weighted image (TR/TE 4,000/92 ms) shows normal length of the urethra (*arrows*) and normal position of a well-supported urethra entirely placed above the inferior pubis level. *P* pubis. **C** Axial T2-weighted image (TR/TE 4,000/92 ms) at proximal urethra, 1 cm from the internal meatus, shows a well-defined linear dark structure, anterior periurethral ligament (PEL—*black arrows*) attaching firmly together with the puborectalis muscle (*arrowheads*). Note symmetric vaginolevator attachments where the PEL and puborectalis muscle join (*white arrows*). *U* urethra, *R* rectum, *EV* endovaginal coil. **D** Axial magnified T2-weighted image at proximal urethra (as in **C**) shows anterior PEL (*arrows*) and lateral paraurethral ligaments (*arrowheads*). **E** Axial T2-weighted image at midurethra, 1.6 cm from the internal meatus, shows anterior PEL and also a posterior ligament (*arrows*) between the urethra (*U*) and vagina (*EV*) that spans between the puborectalis muscle attachments. **F** Axial T2-weighted image at distal urethra, 2.5 cm from internal meatus, shows anterior parallel pubourethral ligaments (*arrows*) extending from the pubis to PEL. **G** Axial T2-weighted image at urogenital diaphragm level, 3.5 cm from internal meatus, shows T2 dark signal of urethrovaginal sphincter muscle (*arrows*), extending around the urethra (*U*) and vagina (*EV*).

Vesicopelvic and urethropelvic fascia provide anterior and lateral support to the bladder neck and urethra by means of attachment to the pubic bone and arcus tendineus fascia pelvis. The endopelvic fascia has condensations forming ligaments of the supporting system of the urethra. MR imaging allows visualization of those ligaments [16–18]. Three groups of ligaments supporting the urethra have been described. The anterior support ligaments include the periurethral ligament (PEL), a thin hypointense structure originating from the medial aspects of the puborectalis muscle and coursing ventrally to the urethra (Fig. 1), and the anterior pubourethral ligaments, paired ligaments extending from the pubis to the anterior aspect of PEL, best seen on axial or sagittal MR images (Fig. 1). The lateral ligamentous support is provided by the paraurethral ligaments which are slightly oblique hypointense thin structures connecting the lateral wall of urethra to the periurethral ligament [18]. The posterior support of the urethra is provided mainly by the vagina. There are fibers that connect the vagina to the puborectalis portion of the levator ani muscle (Fig. 1), the vaginolevator attachment. The vaginolevator attachment is formed by the fibrous tissue and smooth muscle of the vaginal wall which is inserted into the body of the puborectalis muscle. The urethra is inseparable from the anterior vaginal wall for the distal half of its course. Along the proximal half of the urethra, the dorsal support is also provided by a ligamentous

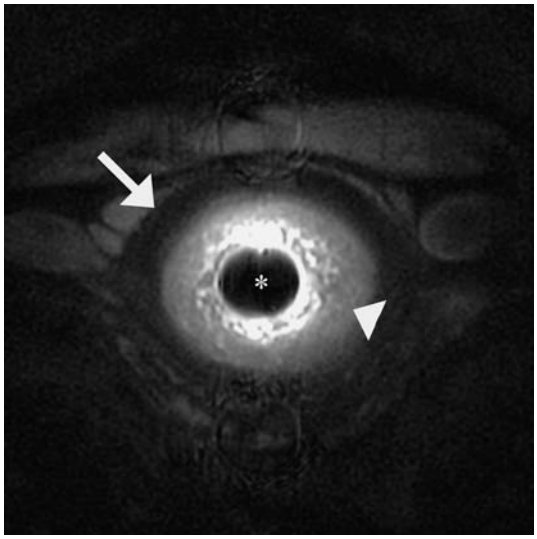

Fig. 2 A 22-year-old continent woman volunteer. Image obtained with 14F endourethral MR coil (Surgi-Vision, Inc. Gaithesburg, MD, USA) on 1.5T GE scanner (Signa LX). Axial T2-weighted image (TR/TE 5,000/63 ms) of the midurethra, 1.5 cm from the internal meatus, shows well-defined T2-dark outer striated sphincter muscle (*arrow*) and high signal inner smooth muscle (*arrowhead*). *Asterisk* represents 14F endourethral coil.

hypointense structure traversing between the vagina and posterior wall of the proximal urethra and connecting to the levator ani at vaginolevator attachment point. This posterior periurethral ligament provides an additional hammock structure for the posterior support of urethra and is best seen on high-resolution axial endovaginal MR images (Fig. 1). Increases in abdominal pressure compress the urethra against the vaginal wall, which acts as a supporting hammock [19]. Lateral detachment of the paravaginal fascial connections from the pelvic wall is associated with stress incontinence and anterior prolapse (cystocele resulting from the abnormal bladder descent) when the firm vaginal support is lost and the compressive force from the vagina on the urethra diminishes.

Functional evaluation of the urethra—urodynamics

Urodynamic tests are the most important functional tests in urinary dysfunction. The purpose of urodynamic assessment is to determine the etiology of incontinence and to evaluate detrusor function. The parameters that are measured during an urodynamic procedure include: pressures (in the bladder and urethra), urine flow, and electromyography (EMG) of the pelvic floor muscle. The cystometrogram is performed to evaluate the compliance and stability of the detrusor muscle. Compliance is simply the elastic property of the detrusor muscles. An evaluation of compliance is an evaluation of the ability of the bladder to "stretch" to "normal" capacity while maintaining low pressures. Stability is evaluated by observing the detrusor while filling the bladder to normal capacity. The evaluation determines the presence or absence of detrusor instability. Vesical pressure is the pressure that is measured with a catheter placed inside the bladder. The pressure is a combination of the pressure being exerted on the bladder by the abdominal contents, the weight or pressure of any urine in the bladder and the force that the detrusor muscle is exerting on that fluid. Abdominal pressure is measured by placing a catheter either in the rectum or the vagina. Abdominal pressure is significant because the bladder is contained by the floor of the abdominal cavity, and it is important to isolate pressures occurring in the bladder itself. For the patient to remain dry, the pressure in the urethra should be equal or greater than the vesical pressure, during bladder filling. The maximum urethral closure pressure for women under the age of 50 is on average 70 cm H_2O, whereas for women aged over 80 it is 24 cm H_2O [20]. When the bladder and urethra are in their proper anatomical location above the pelvic floor level, any pressure increases in the abdominal cavity, from strain or any other cause, will be reflected in both the vesical and urethral pressures, keeping the pressures in the urethra greater than the pressure in the bladder. With aging, chronically increased intraabdominal pressures with coughing, or after childbearing, pelvic surgeries, the female pelvic floor defects can cause the bladder neck and urethra to fall below the pelvic floor level. Increase in abdominal pressures during a Valsalva will lead to pressures in the bladder being higher than in the urethra. This results in urine leakage with increasing abdominal pressures or stress incontinence [21]. Video-urodynamics by simultaneous registration of pressure in the bladder and rectum, and visualizing on fluoroscopy the bladder cycle through the filling and emptying phases provide additional information by generating radiographs representative of functional states during voiding that can be directly correlated with pressure changes.

Cystourethrography and ultrasound

Voiding cystourethrography (Fig. 3) is used to evaluate the anatomical integrity and relationships of the bladder and urethra. It allows the evaluation of the bladder neck and urethral mobility during voiding, and detects cystoceles (bladder prolapse) related to support defects. The exam involves catheterization of the bladder and retrograde filling of the bladder with contrast, and subsequent monitoring and documentation of bladder descent and urethra mobility during voiding.

Ultrasonography is inexpensive, easy to apply and non-invasive technique free of radiation exposure that has been successfully utilized in the evaluation of the urethrovesical junction in stress urinary incontinence.

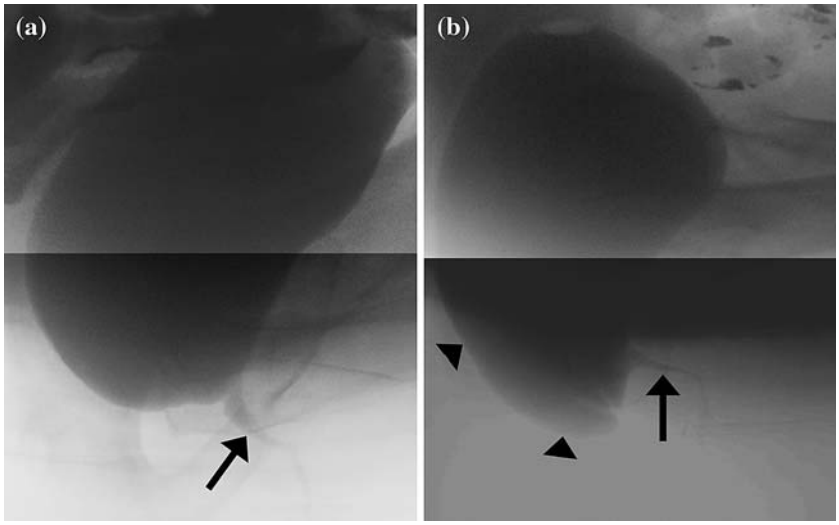

Fig. 3 Cystourethrography. **A** 76-year old woman with well supported bladder. Lateral view shows normal orientation of the urethra during voiding (*arrow*). **B** 67-year old woman with urinary incontinence. Lateral view during voiding shows hypermobile urethra displaced into a horizontal position (*arrow*) and 2 cm cystocele (*arrowheads*).

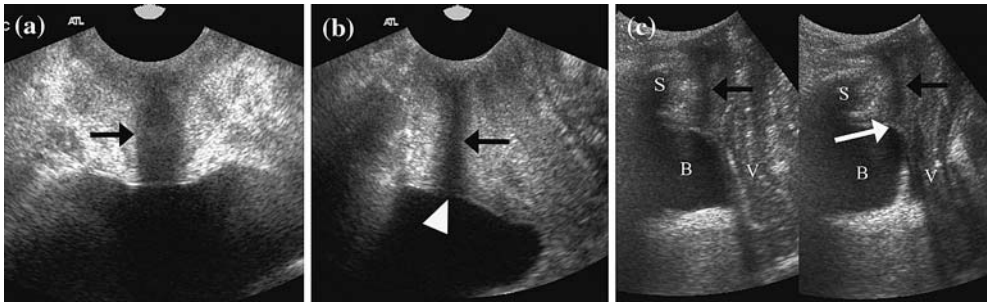

Fig. 4 Ultrasound of the urethra in a 62-year old woman with UTIs and no urinary incontinence. **A** Endovaginal ultrasound image of the urethra in coronal plane shows hypoechoic urethra (*arrow*). **B** Sagittal view shows urethra (*arrow*) and bladder neck (*arrowhead*) at rest. **C** Transperineal ultrasound image in sagittal plane during rest (*left*) and strain (*right*) shows minimal mobility of the urethra (*black arrow*) and intact bladder neck (*white arrow*). *B* bladder. *V* vagina. *S* symphysis pubis.

Ultrasound allows direct visualization of the urethra (Fig. 4) and can be used to assess urethral muscle thickness [22] and volume, bladder neck mobility and competence at rest and during strain [23, 24]. Ultrasound may help in documenting bladder prolapse, urethral hypermobility and bladder neck insufficiency—funneling [23]. High-resolution intraurethral ultrasound was investigated [22] and provided excellent cross-sectional images that allow for real-time visualization of the urethral rhabdosphincter. Urethra support mechanism, however, can only be evaluated indirectly with ultrasound based on the urethral motion, as the ligaments supporting the urethra cannot be visualized with ultrasound.

MR imaging of urethra

MR imaging with its high soft tissue contrast resolution allows the visualization of the urethra and its supporting structures with great detail, and also permits the evaluation of urethral mobility and bladder neck competence during strain and Valsalva. The position and mobility of the anterior vagina, bladder, and urethra are important to urinary continence and anterior prolapse. At rest the urethral axis is vertical and in continent women positioned above the level of pelvic diaphragm. With increasing abdominal pressure and laxity of the pelvic floor and urethral attachments, there is rotational descent of the urethra (Fig. 5). When the urethral axis rotates over 30°, it is defined as UH. Urethral mobility is tested clinically with the Q-tip test [25]. The Q-tip test is performed by inserting a lubricated sterile cotton-tipped applicator into the bladder to the level of vesical neck; the resting angle is recorded. The patient is asked to strain, and the degree of rotation is assessed. UH is defined clinically as a resting or straining angle of greater than 30° from the horizontal, in a patient in lithotomy position. MR imaging is able to demonstrate not only the hypermobility of urethra, but also other associated findings. UH of the urethra is often accompanied by moderate to severe bladder descent with anterior bulging of the vagina (anterior prolapse—cystocele). In severe cases, the anterior vagina can even protrude through the introitus.

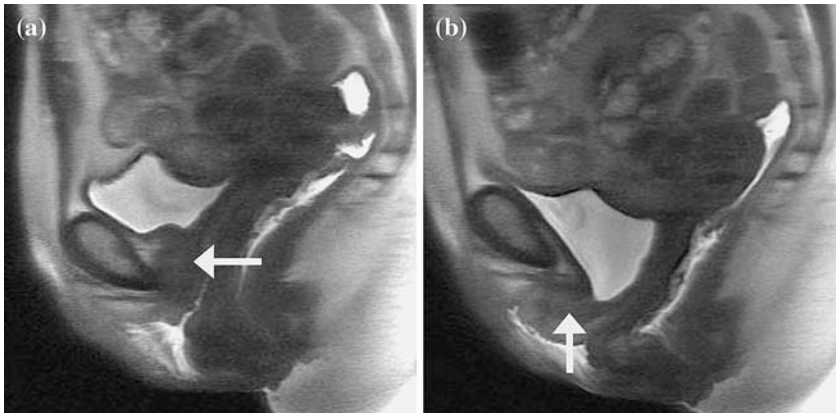

Fig. 5 A 59-year-old woman with urinary incontinence and defecatory dysfunction. **A** Sagittal SSFSE image (TR/TE 15,000/78 ms) at rest shows vertical position of the urethra (*arrow*). **B** Sagittal SSFSE image during strain shows hypermobility of the urethra which is manifested by a rotational descent of the urethra into a horizontal position (*arrow*).

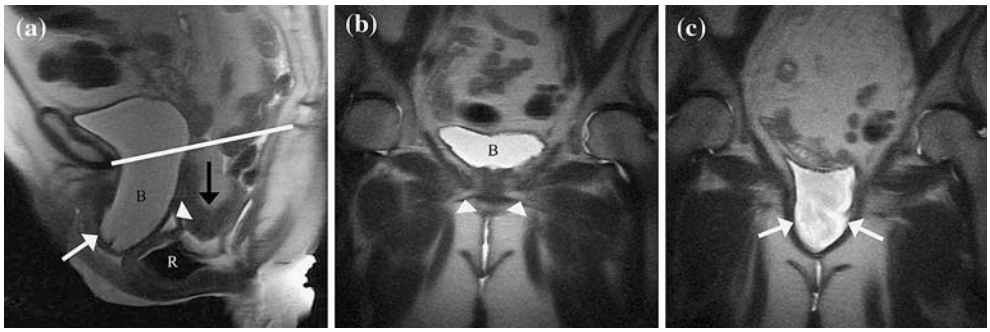

Fig. 6 A 76-year-old woman with pelvic organ prolapse. **A** Sagittal SSFSE image (TR/TE 2,015/76 ms) shows hypermobility of the urethra and a large cystocele (*white arrow*). Note marked displacement of the bladder (*B*), vaginal apex (*arrowhead*), rectum (rectocele *R*), and cul-de-sac with bowel (*black arrow*) below the level of pubococcygeal line (a line drawn from the inferior pubis to the last visible coccygeal joint). **B** Coronal SSFSE image (TR/TE 2,045/60 ms) shows at rest the normal position of bladder (*B*) above the level of pelvic floor (*arrowheads*). **C** Coronal SSFSE image (TR/TE 2,045/60 ms) shows during strain a cystocele (*arrows*) extending below the level of pelvic floor.

On MR imaging, urethral and bladder descent are assessed in reference to the level of the pelvic floor which can be defined by a pubococcygeal line (PCL) extending from the most inferior portion of the symphysis pubis to the sacrococcygeal joint [26, 27]. The pubococcygeal line can also be drawn from the inferior pubic symphysis to the last coccygeal joint or the junction of the first and second coccygeal segments on a midsagittal image [28, 29] (Fig. 6). Components of the pelvic floor support, such as the pubo-coccygeus muscle attach along this line. The advantage of this reference line is that it can be reproduced easily in all patients, and it is independent of the pelvic tilt. The degree of descent of the pelvic organs within the three pelvic compartments can be evaluated in reference to PCL as the vertical distance between the resting and strain positions of the urinary bladder neck, the cervix or vaginal apex, and the anorectal junction. Cystocele is defined as a descent of the bladder base below inferior margin of the pubic bone or below PCL, either at rest or during strain (Fig. 6). Cystocele is measured as a vertical distance between the PCL and the most inferior portion of the bladder. Yang et al. [26] demonstrated that the normal vertical distance from PCL to the bladder base at strain should be not more than 1 cm below the line.

Other findings associated with UH that can be detected on MR imaging are distortion of urethral support ligaments, either partial or complete. Partial defects include laxity, fluttering or focal attenuation of ligaments. Complete disruption shows a discontinuity of ligamentous fibers [17, 18]; mostly affected and reproducibly visualized on imaging is PEL. Findings are frequently accompanied by the abnormal vaginal configuration (loss of normal H-shape vaginal contour, or dropping vaginal fornix), best seen on axial images, and widening of para-vaginal attachments (Figs. 7, 8).

The levator ani muscle signal and integrity can be well evaluated on MR images, on axial and coronal T2-weighted images. Levator ani should be symmetric without defects or fraying. Abnormal signal in the levator muscle, when compared to the obturator internus, and thinning can be observed in patients with stress incontinence and can be a result of fatty infiltration and atrophy as well as direct muscle injury [29]. The normal thickness of the puborectalis muscle is 5–6 mm [30]. Interruption of the muscle fibers, lateral deviation of the

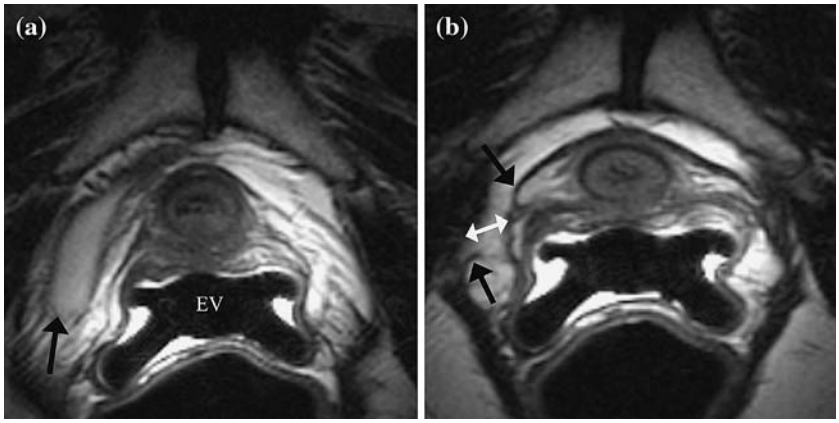

Fig. 7 A 54-year-old woman with urinary incontinence. **A** Axial T2-weighted image (TR/TE 4,000/92 ms) at proximal urethra shows asymmetric right bladder base laxity (*arrow*). *EV* endovaginal coil. **B** Axial T2-weighted image at midurethra shows disruption of the right PEL and vaginolevator attachments (*black arrows*). Note asymmetric widening of the space between the puborectalis muscle and right lateral vaginal wall (*white arrows*), when compared to the left side.

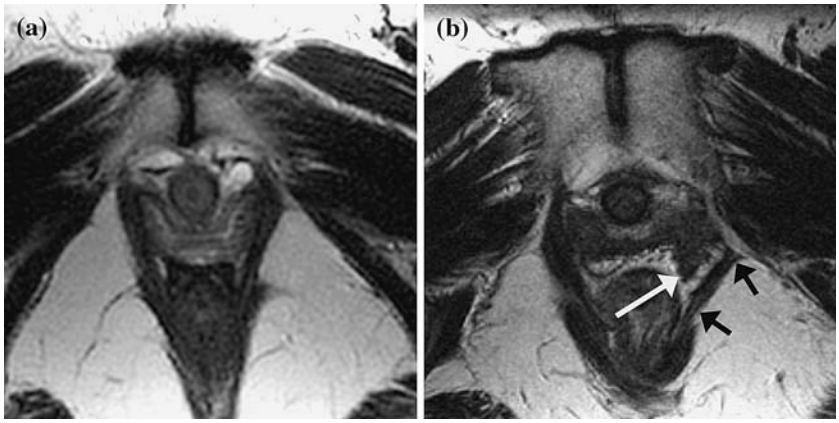

Fig. 8 Comparison between the vaginal configuration with intact vaginolevator attachments and with paravaginal tears. **A** Normal symmetric H-shaped vagina in a 35-year-old continent woman. **B** Disrupted vaginal attachments on the left resulting in drooping vagina (*white arrow*) in a 47-year-old woman with urinary incontinence. Note asymmetric thinning of the left puborectalis muscle (*black arrows*) which also has a lateral deviation, when compared to that of the right.

muscle that is frequently associated with vaginal shape distortion on the affected side, can be observed (Fig. 8).

In patients with UI who do not show signs of pelvic floor laxity, ISD may be responsible for symptoms. There are some imaging findings that are more likely to be associated with ISD, such as a short urethra, urethral muscle thinning or defect (e.g., diverticulum) or bladder neck weakness demonstrated by funneling. The average length of the urethra in continent patients as evaluated with MR imaging is 3.8 cm (SD 0.3 cm) [12]. When the urethra is shorter than 3.0 cm, or when the segment of the urethra above the pelvic floor level is less than 3.0 cm in length, urethral sphincter weakening can lead to incontinence (Fig. 9). Thinning of the urethral striated muscle has been reported in patients with stress incontinence [18]. It has been shown that ISD can be related to decreasing sphincter muscle volume (Fig. 10); however, the quantity of striated muscle also decreases with normal aging. Diverticulum may cause incontinence by weakening the sphincter wall. Urethral diverticulum occurs due to infection of the paraurethral glands, and may or may not communicate with the urethral lumen. Diverticulum in the midurethra usually does not cause UI if the proximal sphincter is intact (Fig. 11). Funneling at the bladder neck, which is the opening of the urethrovesical junction

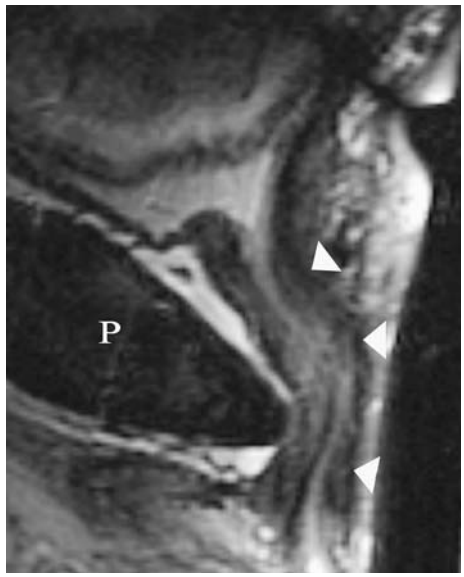

Fig. 9 A 66-year-old woman with urinary incontinence. Sagittal T2-weighted image (TR/TE 4,000/92 ms) shows normal total length of the urethra (*arrowheads*); however, about 1/3 of the urethra is positioned below the pubis level, compatible with weak urethral support. Compare to normal support of the urethra shown in Figure 1B. *P* pubis.

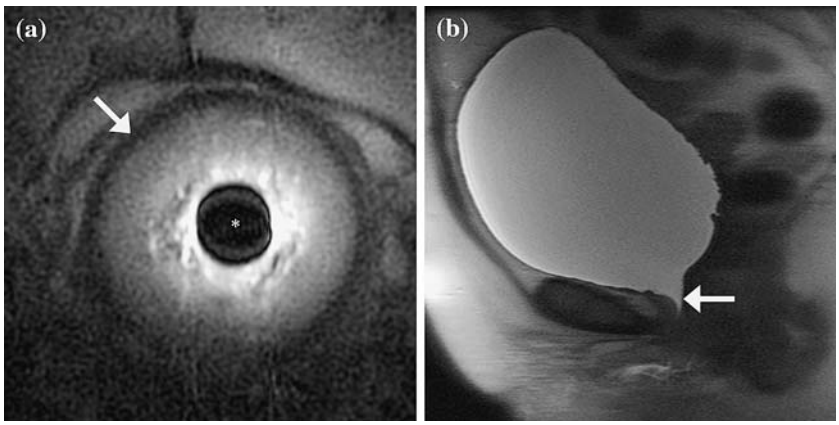

Fig. 10 A 63-year-old woman with urinary incontinence. **A** Axial T2-weighted image (TR/TE 5,000/69 ms) of the midurethra shows a well-defined T2-dark outer striated sphincter muscle (*arrow*) which is very thin. *Asterisk* respresnts 14F endourethral coil. **B** Sagittal SSFSE image (TR/TE 15,000/78 ms) shows marked funneling of bladder neck (*arrow*) with the full bladder at rest. Funneling at rest strongly suggests ISD.

Fig. 11 A 56-year-old woman with urethral diverticulum. **A** Axial T2-weighted image (TR/TE 5,000/99 ms) shows a fluid intensity diverticulum (*arrow*) encircling the *right side* of the urethra.

at rest or during strain, can be seen on MR imaging in patients with UI (Fig. 10). An open bladder neck and proximal urethra at rest or strain was shown to indicate an ISD [21]; however, funneling can be also found in some postmenopausal continent women.

MR imaging protocol

Urethral anatomy is best evaluated on T2-weighted images obtained in three orthogonal planes. To achieve the highest resolution and SNR, endocavitary coils can be used [17]. Endovaginal or endorectal coil used with the small field of view, thin slices, and high imaging matrix allow detailed assessment of periurethral anatomy (e.g., periurethral ligament PEL) that can be obscured because of a partial volume averaging effect when imaged with a standard pelvic phased array coil or when imaged in the plane that is not perpendicular to the urethra. The intraurethral coil allows the assessment of the urethral sphincter muscle integrity, as both the smooth and striated muscles are well seen [12]; however, because of its limited anatomical coverage with significant signal drop within 2–3 cm from the coil placed in the urethra lumen, only a small portion of the anatomy can be evaluated with the intraurethral approach. To assess the urethral function during strain, to detect cystocele and to evaluate the levator ani muscles, imaging with the pelvic phased array coil proves to be optimal. Single shot fast spin echo techniques (SSFSE/HASTE) can be used for dynamic pelvic floor imaging when the bladder neck and urethral motion can be registered and subsequently reviewed using a cine display. An example of the imaging protocol for the evaluation of the female urethra is presented in Table 1.

Summary

Sphincteric urinary incontinence is related to urethral hypermobility (UH) and intrinsic sphincter deficiency (ISD). Imaging plays an adjunct role to urodynamics in the assessment of women with UI. MR imaging due to its superior soft tissue contrast resolution contributes many findings that are predictive of UH, where the basic abnormality is weakness of pelvic floor support, such as abnormal descent of the bladder neck, disruption of periurethral ligaments and vaginal attachments, and defects within the levator ani muscle. In ISD, where there is weakness and malfunction of urethral sphincter itself, MR imaging may show foreshortening or thinning of the sphincter muscle and bladder neck insufficiency manifested by funneling. Some patients may demonstrate imaging findings of both UH and ISD, as the ISD with bladder neck funneling may represent a secondary deficiency related to abnormal proximal urethral wall traction and shearing that can overcome urethral coaptation in chronic hepermobility [31]. Currently, MR imaging is considered in the diagnostic work-up of women who failed prior surgeries for incontinence or who have severe and complex pelvic organ prolapse. As we learn more about specific anatomical defects related to UI that can be observed on MR images, the role of MR imaging in primary diagnosis of patient with stress UI is expected to increase.

Table 1 Example of MR imaging protocol to evaluate patients with UI at 1.5T

Coil(s)	Endo rectal or vaginal	Endo rectal or vaginal	Endo rectal or vaginal	Pelvic phased array	Pelvic phased array	Pelvic phased array
Sequence	T2 hi-res FSE	T2 hi-res FSE	T2 hi-res FSE	T2 FSE	T2 FSE	SSFSE[c]
Imaging plane	Sagittal	Axial[a]	Coronal	Axial	Sagittal	Sagittal, coronal
Anatomic coverage	Pubis to rectum	Bladder to below pubis	Hip to hip	Aortic bifurcation below symphysis pubis	Pubis to sacrum	Bladder/urethra dynamic sequence with strain
TE (ms)	90–120	90–120	90–120	90–120	90–120	70
TR (ms)	4000–6000	4000–6000	4000–6000	4000–6000	4000–6000	15,000∞
Slice thickness/spacing (mm)	3/0-1	3/0-1	3/0-1	4-6/0-1	4-6/0-1	6/1
Field of view (cm)	10–14	10–14	10–14	20	20	25–30
Frequency direction	AP or SI	AP[b]	AP or SI	Transverse	SI	SI
Matrix	256 × 192	256 × 192	256 × 192	512 × 512	512 × 512	512 × 512
NEX	3–4	3–4	3–4	1–2	2	0.5

[a]Axial oblique plane perpendicular to the urethral axis
[b]Frequency direction AP to avoid endorectal/vaginal coil motion artifact over the urethra
[c]Series at rest followed by repeat series during strain (can be imaged in axial, sagittal and coronal planes)

Acknowledgment. Work presented in this article was partially supported by the Seed Grant from the Radiological Society of North America and the Young Investigator Award from the Society of Computed Body Tomography and Magnetic Resonance received by KJM.

References

1. Abrams P, Blaivas JG, Stanton SL, Anderson JT (1998) The standardization of terminology of lower urinary tract function. Scand J Urol Nephrol 114(Suppl):5–19
2. Blaivas JG, Romanzi LJ, Heritz DM (1997) Urinary incontinence: pathophysiology, evaluation, treatment overview, and nonsurgical management. In Walsh PC, Retik AB, Vaughan ED, Wein AJ (eds). *Campbell's Urology*. Philadelphia: WB Saunders, pp 1007–1043
3. McGuire EJ, Fitzpatrick CC, Wan J, Bloom D, Sanvordenker J, Ritchey M, Gormley EA (1993) Clinical assessment of urethral sphincter function. J Urol 150:1452–1454
4. White RD, McQuown D, McCarthy TA, Ostergard DR (1980) Real-time ultrasonography in the evaluation of urinary stress incontinence. Am J Obstet Gynecol 138(2):235–237
5. Quinn MJ, Beynon J, Mortensen NJ, Smith PJ (1988) Transvaginal endosonography: a new method to study the anatomy of the lower urinary tract in urinary stress incontinence. Br J Urol 62(5):414–418
6. Richmond DH, Sutherst JR (1989) Clinical application of transrectal ultrasound for the investigation of the incontinent patient. Br J Urol 63(6):605–609
7. Athanasiou S, Khullar V, Boos K, Salvatore S, Cardozo L (1999) Imaging the urethral sphincter with three-dimensional ultrasound. Obstet Gynecol 94(2):295–301
8. Klein HM, Kirschner-Hermanns R, Lagunilla J, Gunther RW (1993) Assessment of incontinence with intraurethral US: preliminary results. Radiology 187(1):141–143
9. Kirschner-Hermanns R, Klein HM, Muller U, Schafer W, Jakse G (1994) Intra-urethral ultrasound in women with stress incontinence. Br J Urol 74(3):315–318
10. Aronson MP, Bates SM, Jacoby AF, Chelmow D, Sant GR (1995) Periurethral and paravaginal anatomy: an endovaginal magnetic resonance imaging study. Am J Obstet Gynecol 173(6):1702–1708
11. Nurenberg P, Zimmern PE (1997) Role of MR imaging with transrectal coil in the evaluation of complex urethral abnormalities. Am J Roentgenol 169(5):1335–1338
12. Macura KJ, Genadry R, Borman TL, Mostwin JL, Lardo AC, Bluemke DA (2004) Evaluation of the female urethra with intraurethral magnetic resonance imaging. J Magn Reson Imaging 20:153–159
13. De Lancey JOL (1986) Correlative study of paraurethral anatomy. Obstet Gynecol 68(1):91–97
14. Oelrich T (1983) The striated urogenital sphincter muscle in the female. Anat Rec 205:223–232
15. Gosling JA (1996) The structure of the bladder neck, urethra and pelvic floor in relation to female urinary continence. Int Urogynecol J Pelvic Floor Dysfunct 7(4):177–178
16. Tan IL, Stoker J, Zwamborn AW, Entius KA, Calame JJ, Lameris JS (1998) Female pelvic floor: endovaginal MR imaging of normal anatomy. Radiology 206:777–783
17. Macura KJ, Genadry RR, Bluemke DA (2006) MR imaging of the female urethra and supporting ligaments in assessment of urinary incontinence: spectrum of abnormalities. Radiographics 26:1135–1149
18. Kim JK, Kim YJ, Choo MS, Cho KS (2003) The urethra and its supporting structures in women with stress urinary incontinence: MR imaging using an endovaginal coil. AJR Am J Roentgenol 180:1037–1044
19. DeLancey JOL (1994) Structural support of the urethra as it relates to stress urinary incontinence: the hammock hypothesis. Am J Obstet Gynecol 170:1713–1723
20. Wang AC, Chen MC (2002) A comparison of urethral pressure profilometry using microtip and double-lumen perfusion catheters in women with genuine stress incontinence. Int J bstet Gynaecol 109:322–326
21. Mostwin JL (1995) Urinary incontinence. J Urol 153(2):352–353
22. Klauser A, Frauscher F, Strasser H, Helweg G, Kolle D, Strohmeyer D, Stenzl A, zur Nedden D (2004) Age-related rhabdosphincter function in female urinary stress incontinence: assessment of intraurethral sonography. J Ultrasound Med 23(5):631–7
23. Cassado J, Pessarrodona A, Tulleuda R, Cabero L, Valls M, Quintana S, Rodriguez-Carballeira M (2006) Introital ultrasonography: a comparison of women with stress incontinence due to urethral hypermobility and continent women. BJU Int 98(4):822–828
24. Huang WC, Yang JM (2003) Bladder neck funneling on ultrasound cystourethrography in primary stress urinary incontinence: a sign associated with urethral hypermobility and intrinsic sphincter deficiency. Urology. 61(5):936–941
25. Bergman A, McCarthy TA, Ballard CA, Yanai J (1987) Role of the Q-tip test in evaluating stress urinary incontinence. J Reprod Med 32:273–275
26. Yang A, Mostwin JL, Rosenshein NB, Zerhouni EA (1991) Pelvic floor descent in women: dynamic evaluation with fast MR imaging and cinematic display. Radiology 179:25–33
27. Gufler H, DeGregorio G, Allmann KH, et al. (2000) Comparison of cystourethrography and dynamic MRI in bladder neck descent. J Comput Assist Tomogr 24:382–388
28. Goh V, Halligan S, Kaplan G, et al. (2000) Dynamic MR imaging of the pelvic floor in asymptomatic subjects. Am J Roentgenol 174:661–666
29. Tunn R, Paris S, Fischer W, et al. (1998) Static magnetic resonance imaging of the pelvic floor muscle morphology in women with

stress urinary incontinence and pelvic prolapse. Neurourol Urodyn 17:579–589
30. Singh K, Reid WM, Berger LA (2002) Magnetic resonance imaging of normal levator ani anatomy and function. Obstet Gynecol 99:433–438
31. Mostwin JL, Genadry R, Saunders R, et al. (2001) Stress incontinence observed with real time sonography and dynamic fastscan magnetic resonance imaging—insights into pathophysiology. Scand J Urol Nephrol Suppl 207:94–99